

An Auxiliary Gravitational Field Operating in Galaxies (Revised)

R. Wayte

29 Audley Way, Ascot, Berkshire SL5 8EE, England, UK.

E-mail: rwayte@googlemail.com

Submitted to vixra 24 October 2019

Abstract: A theory has been developed of an auxiliary gravitational field which operates in conjunction with relativistic gravity and accounts for the empirical success of Milgrom's modified Newtonian dynamics theory. Remarkable links between this astronomical theory and atomic physics have been discovered. Resonant, standing-wave properties of the field encourage the formation of flat rotation curves, bar or spiral structures and quantised galactic rings. Gravitational lensing due to this field is also significant. The angular momentum proportional to mass-squared relationship observed in galaxies is attributed to this field selecting a preferred galactic rotation velocity.

PACS Codes: 04.60.Bc, 95.35.+d, 98.62.Dm

1. Introduction

An auxiliary gravitational field will be prescribed which operates *in addition to* normal gravity without modifying General Relativity theory or Newtonian dynamics yet reducing the amount of dark matter required in galaxies. This relativistic theory will fully incorporate the empirical successes of MOND and also possess physical attributes which *determine* the main characteristics of spiral galaxies. It does not exclude the possibility of some dark matter in galaxies, clusters or inter-cluster space, necessary to satisfy the standard cosmology model. But, dark matter has never been seen and its theory is grossly inelegant for describing the dynamics of galaxies.

Milgrom and others have applied his theory of modified Newtonian dynamics (MOND) to galaxies and clusters of galaxies with impressive success as a neat alternative to the dark matter hypothesis [1-14]. It is empirical and has been proposed as a modification to the Newtonian law of gravity or of inertia. However, although MOND satisfies the Tully-Fisher law [15] and *describes* rotation curves very well, it cannot actually *dictate the distribution* of matter within a disc galaxy any more than standard

gravitation theory can. Therefore, flat rotation curves are *not* imposed by MOND, neither are density variations within galactic rings or spirals and bar structures.

The field theory developed herein goes well beyond Milgrom's MOND or subsequent relativistic theories by Bekenstein [16] and Moffat [17, 18]. It explains the observed structure within galaxies in addition to reducing the need for dark matter. Characteristics of the field are defined as follows:

(a) Orbiting atoms are induced by the normal radial gravitational field to emit an azimuthal energetic quantum field around their orbit analogous to electromagnetic virtual photons. (b) The attractive interaction of this orbiting field with the normal radial field produces the extra binding gravitational force observed in galaxy dynamics. (c) The orbiting field has a quantised resonant standing-wave nature which *causes* galactic material to form into flat rotation curves with bars or spirals and segments, and also to prefer quantised dimensions for galactic rings. (d) The field is easily destroyed by turbulence and may not have developed completely in unsettled galaxies, or not at all in irregular galaxies: it will only be seen optimised in calm rotating systems. These features make the field reminiscent of a binding cordeliere, hence *gravito-cordic field*.

2. The characteristic acceleration factor

As for MOND, a characteristic acceleration factor a_0 is to be fundamental to this gravito-cordic field, and it will be seen to relate galactic to atomic dimensions as follows. First, we have a basic relationship between observable galaxy mass M and asymptotic rotation velocity V_∞ in Keplerian circular orbits:

$$a_0 GM = V_\infty^4 . \quad (2.1)$$

Second, we shall see in Section 7 that there is an optimum galactic material velocity for gravito-cordic field production; that is, $V_{201} = 201 \text{ kms}^{-1} = (4\pi\alpha^2)c$, where $\alpha \sim 1/137$ is the atomic fine structure constant and c is the velocity of light. Third, an associated *gravitational de Broglie wavelength* (λ_{GH}) due to hydrogen electrons can then be matched to a characteristic galactic mass ($M_G = 1.09 \times 10^{11} M_\odot$) by:

$$\lambda_{GH} = \left(\frac{h}{mV_{201}} \right) \times 137 \times \left(\frac{E}{G} \right)^{1/2} = 2\pi \left(\frac{GM_G}{c^2} \right) \quad ; \quad (2.2)$$

where m is electron mass, h is Planck's constant, and $(E/G = e^2/Gm^2)$ is the ratio of electric to gravitational force. Thus, for these optimum conditions, (2.1) yields:

$$a_o = (V_{201})^4 / GM_G = 1.116 \times 10^{-10} \text{ ms}^{-2} \quad , \quad (2.3a)$$

which is within the range suggested by the MOND observations and does not look like some random coincidence. For Keplerian motion [$GM_G = (V_{201})^2 R_G$] a corresponding radius ($R_G = 11.7 \text{ kpc}$) may also be involved through:

$$a_o = GM_G / R_G^2 = (V_{201})^2 / R_G \quad , \quad (2.3b)$$

so a_o is the acceleration at radius R_G when galactic mass M_G is included.

This empirical result is very satisfactory from an astronomy point of view but it must ultimately be founded upon a source process to do with atomic hydrogen. One such exact and compelling connection with the 1st Bohr orbit of hydrogen follows from introducing (2.2) into (2.3a):

$$a_o = \left(\frac{v_1^2}{r_1} \times 137^2 \right) \times (4\pi\alpha^2)^5 \times \left(\frac{G}{E} \right)^{1/2} = 1.116 \times 10^{-10} \text{ ms}^{-2} . \quad (2.4a)$$

Here, the first bracket contains the acceleration of the orbiting electron around the proton, with velocity ($v_1 = c/137$) at radius r_1 . Velocity ($137v_1 = c$) also matches the propagation velocity of the gravito-cordic field emitted by the electron. The second bracket contains the velocity factor for optimum field production and propagation mentioned above. A further interesting connection with the 1st Bohr orbit is then a scale factor:

$$R_G = r_1 \times \left[(E/G)^{1/2} / (4\pi\alpha^2)^3 \right] . \quad (2.4b)$$

Hydrogen atoms are therefore considered to be the most prolific source of the gravito-cordic field. Relationships like these between atoms and galaxies have never been seen before and are a sign that gravity is electromagnetic. At present, the galactic dark matter alternative hypothesis relies totally upon the proposed existence of unspecified exotic particles.

3. Some fundamental relationships

The *asymptotic* acceleration formula for total *observed* acceleration g at radius R is given in MOND by:

$$g = \left(\frac{GM}{R^2} a_o \right)^{1/2} = (g_N a_o)^{1/2} \quad , \quad (3.1)$$

where g_N is the Newtonian acceleration for *observable* mass M and can be much less than a_o . This has now to be re-interpreted for the real gravito-cordic field because terms like

$g_N^{1/2}$ and $a_o^{1/2}$ are not regular, physically tangible. By introducing (2.3b) this expression becomes:

$$g = a_o \left(\frac{M}{M_G} \right)^{1/2} \left(\frac{R_G}{R} \right) , \quad (3.2)$$

so that variable parameters (M , R) can be normalised with respect to real characteristic values at R_G , and a_o clearly derives from the most fundamental source (2.4a). Likewise, the gravito-cordic binding force acting radially on a test particle m may be better understood as a physical process when it is expressed as:

$$F = mg = m \left(\frac{GM}{R^2} \right)^{1/2} \times \left(\frac{GM_G}{R_G^2} \right)^{1/2} , \quad (3.3)$$

where $(GM/R^2)^{1/2}$ represents *coherence amplitude* in the graviton *intensity* field emitted by all the atoms which constitute central mass M , (this is analogous to summing waves of random phase). It is this amplitude component which induces the orbiting hydrogen to emit the circumferential gravito-cordic field.

One important feature of the gravito-cordic force is that it is not generally reciprocal. If it were, then according to (3.1), the force exerted by our Galaxy (of included mass M_{gal}) on the orbiting Sun (mass M_\odot) would be:

$$F_G = M_\odot \left(\frac{a_o GM_{gal}}{R^2} \right)^{1/2} , \quad (3.4a)$$

whereas the Sun would have to re-act on the whole galaxy with force:

$$F_S = M_{gal} \left(\frac{a_o GM_\odot}{R^2} \right)^{1/2} = F_G \times \left(\frac{M_{gal}}{M_\odot} \right)^{1/2} . \quad (3.4b)$$

Since this effect is definitely not observed, the orbiting Sun must be induced by the Galaxy to emit its orbiting gravito-cordic field whereas the Galaxy is *not* orbiting the Sun and is *not caused* to emit a field. By inference then, the gravito-cordic field energy is confined to its own orbit and there is no interaction between completely independent galaxies other than normal gravity. (Galaxies orbiting within clusters are not independent and will have their own gravito-cordic field between the galaxies). In addition, it also means that the general cosmological expansion of the Universe is not affected. This lack of reciprocity also applies to MOND when it is interpreted as a general modification of gravity, and it also appears very detrimental to Moffat's theory [17,18].

Consequently, the gravito-cordic force exists within a galaxy *in addition* to normal gravity and orbiting bodies experience both forces simultaneously acting towards the galactic centre. The total gravitational acceleration could therefore at first sight be:

$$g_{\omega} = g_N + (g_N a_o)^{1/2} . \quad (3.5)$$

Unfortunately, when this formula is applied to planetary motion in the solar system, the gravito-cordic component is easily strong enough to have been detected if it existed [19]. Therefore, we shall attenuate that component only, in a way to mimic the MOND formula (3.7a), but without modifying the Newtonian gravity term g_N . Fortunately, there is a formula from the theory of electromagnetic inductive coupling [20] which is logically perfect for this attenuation; then:

$$g_{\omega} = g_N + a_o \left\{ \frac{(g_N/a_o)^{1/2}}{[(g_N/a_o) + 1]} \right\} . \quad (3.6)$$

Here, a_o represents a theoretical available acceleration due to the circulating gravito-cordic field. *Factor $(g_N/a_o)^{1/2}$ acts like a coefficient of coupling so that the curly bracket is a **response function** describing how the Newtonian field couples with the gravito-cordic field.* This final field is slightly stronger than the MOND field but it satisfies the solar system criteria and the multitude of galaxy rotation curves already fitted with MOND. Equations (3.6), with (2.1), (2.2) and (2.4a) represent concrete theoretical considerations supporting the auxiliary field postulate.

For comparison, Milgrom's complete MOND formula is usually given by:

$$\left[\frac{g_{\mu}}{(a_o^2 + g_{\mu}^2)^{1/2}} \right] g_{\mu} = g_N , \quad (3.7a)$$

where g_{μ} is the total observed acceleration and g_N is again the calculated Newtonian acceleration for the *observable* mass (stars, gas, dust). This reduces to:

$$g_{\mu} = \left\{ \left(\frac{1}{2} \right) \left[g_N^2 + (g_N^4 + 4a_o^2 g_N^2)^{1/2} \right] \right\}^{1/2} . \quad (3.7b)$$

Moffat's [17,18] alternative theory to MOND has acceleration which may be expressed:

$$g_M = g_N + \left(g_N \frac{GM_o}{r_o^2} \right)^{1/2} \left[\frac{r_o}{r} - \left(1 + \frac{r_o}{r} \right) \exp \left(-\frac{r}{r_o} \right) \right] , \quad (3.8)$$

for M_o and r_o as arbitrary best-fit parameters. Strangely, this conscripts a *repulsive* Yukawa potential component to oppose an attractive $M^{1/2}$ term.

4. Application to galaxies and clusters

Figure 1 illustrates the variation of the above expressions for g_N , g_μ , g_ω , and g_M , with normalised radius. Clearly, the asymptotic relationship (2.1) holds for g_ω as for g_μ , so Milgrom's many published calculations of rotation curves for disc galaxies will remain valid, but the mass distribution will change a little by moving some matter outwards from the centre. For example, at the radial position where $g_N = a_0$ and $R = R_G$, we have ($g_\omega = 1.5g_N$) compared with Milgrom's ($g_\mu = 1.27g_N$), so the included mass must be 1.18 times less for a given rotation velocity. Moffat's theory produces a field strength which is 1.33 times greater than Milgrom's if his suggested values are used ($M_0 = 10^{12} M_\odot$, and $r_0 = 13\text{kpc}$). Kent [21-23] has fitted maximum-disk solutions to many disk galaxy rotation curves by carefully selecting best-fit M/L ratios, which are large enough to cover the presence of a gravito-cordic field and some dark matter.

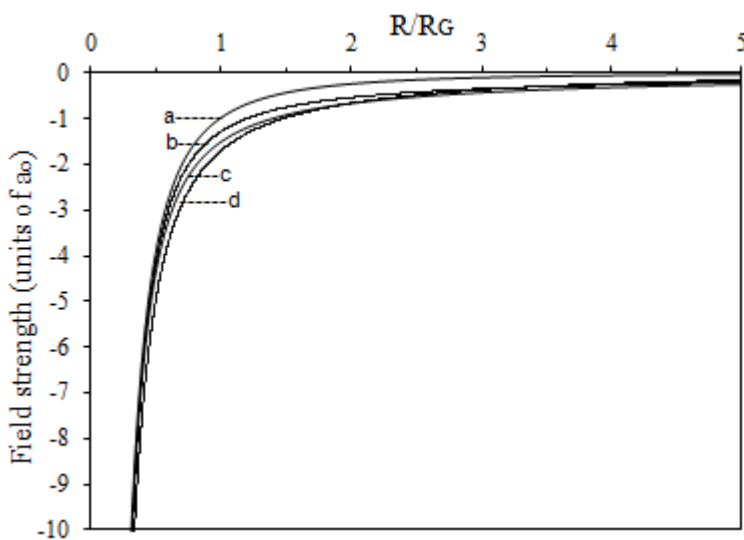


Figure 1. Comparison of accelerations versus normalised radius
(a) g_N , (b) g_μ , (c) g_ω , and (d) g_M .

When applied to clusters of galaxies which are supported by angular momentum, MOND theory is still very effective but appears to leave a virial discrepancy amounting to a deficiency factor of 2 in observable matter, [5, 6]. This discrepancy could be reduced by up to 15% if g_ω were used instead of g_μ . Therefore, some kind of dark matter is still necessary in these systems.

Work done by Brownstein & Moffat [24] on galaxy-cluster masses without dark matter has indicated that MOND cannot be applied to isotropic thermal models of

clusters which are only supported by gas pressure. This exclusion also applies to our gravito-cordic field which can only be generated by orbiting matter.

5. Aspects of a relativistic field

Einstein's equations are a mathematical description of *any* conserved energetic field so they can be applied to a conserved gravito-cordic field with or without the normal radial gravitational field.

Consider an idealised disk galaxy in which surface mass density has been observed to be exponential with radius, namely:

$$\rho_s = \rho_o \exp(-r/r_c), \quad (5.1a)$$

where r_c is the characteristic radius. Then, the galactic mass distribution is given by integration:

$$M = \int_0^r 2\pi r \rho_s dr = M_{\max} \left[1 - \left(1 + \frac{r}{r_c} \right) \exp\left(-\frac{r}{r_c}\right) \right], \quad (5.1b)$$

where M_{\max} is the total disk mass. Now, by transforming to a sphere, the analysis will be easier yet accurate enough for our purposes. Hence, let this radial mass distribution be equivalent to a spherical galaxy of bulk density:

$$\rho_b = \frac{M_{\max}}{4\pi r_c^2} \left(\frac{\exp-r/r_c}{r} \right), \quad (5.1c)$$

so that Einstein's equations describing the spherically-symmetric static field in polar coordinates can be applied, (see [25] p242). For the line element:

$$ds^2 = -e^\lambda dr^2 - r^2 d\theta^2 - r^2 \sin^2 \theta d\phi^2 + e^\nu dt^2, \quad (5.2)$$

the surviving components of the energy-momentum tensor are:

$$8\pi(G/c^4)\Gamma_1^1 = -e^{-\lambda} \left(v'/r + 1/r^2 \right) + 1/r^2, \quad (5.3a)$$

$$8\pi(G/c^4)\Gamma_2^2 = 8\pi(G/c^4)\Gamma_3^3 = -e^{-\lambda} \left\{ v''/2 - \lambda'v'/4 + v'^2/4 + (v' - \lambda')/2r \right\}, \quad (5.3b)$$

$$8\pi(G/c^4)\Gamma_4^4 = e^{-\lambda} \left(\lambda'/r - 1/r^2 \right) + 1/r^2. \quad (5.3c)$$

Now for an interior field without pressure, suspended by angular momentum, we shall equate the metric tensor components $e^\nu = e^{-\lambda}$. Given that $e^{-\lambda}$ is a potential function, we can express the field strength in the usual way and equate it to the total field in (3.6):

$$\left(\frac{c^2}{2} \right) \frac{d}{dr} \left(e^{-\lambda} - 1 \right) = a_o \left\{ \frac{g_N}{a_o} + \frac{(g_N/a_o)^{1/2}}{[(g_N/a_o) + 1]} \right\}. \quad (5.4a)$$

However, upon introducing mass (5.1b), it is necessary to integrate this numerically to produce an expression for $e^{-\lambda}$ which can be approximated to a simple function. From Kent's work [21-23] we can introduce values for large galaxies ($M_{\max} = 10^{11}M_{\odot}$, $r_c \sim 7\text{kpc}$) such that on average ($GM_{\max}/r_c^2 a_o \sim 2.5$), then for ($R = r/r_c$):

$$\frac{g_N}{a_o} = \left(\frac{GM}{a_o r^2} \right) = \left(\frac{GM_{\max}}{a_o r_c^2} \right) \left(\frac{1}{R^2} \right) [1 - (1+R)\exp(-R)]. \quad (5.4b)$$

Upon introducing this into (5.4a), integration has the approximate form ($0 < R < 5$):

$$\begin{aligned} e^{-\lambda} &= 1 - \left(\frac{2a_o r_c}{c^2 R} \right) \left[11.25 \left(1 + \frac{R}{8.5} \right) (1 - \exp(-R/1.5)) \right] \\ &= 1 - \left(\frac{2GM_{\max}}{c^2 r_c R} \right) \left[4.5 \left(1 + \frac{R}{8.5} \right) (1 - \exp(-R/1.5)) \right]. \end{aligned} \quad (5.4c)$$

This designates infinity as the coordinate reference frame of special relativity, and the negative potential energy at small R is 3 times the Newtonian value alone.

If the Newtonian term is removed from the right side of (5.4a), then only the gravito-cordic field is considered such that integration for $e^{-\lambda}$ has the approximate form ($0 < R < 5$):

$$\begin{aligned} e^{-\lambda} &= 1 - \left(\frac{2a_o r_c}{c^2 R} \right) \left[37.5 \left(1 - \frac{R}{25.5} \right) (1 - \exp(-R/7.5)) \right] \\ &= 1 - \left(\frac{2GM_{\max}}{c^2 r_c R} \right) \left[15 \left(1 - \frac{R}{25.5} \right) (1 - \exp(-R/7.5)) \right]. \end{aligned} \quad (5.4d)$$

This also designates infinity as the coordinate reference frame of special relativity, and the potential energy at small R is 2 times the Newtonian value.

If the gravito-cordic term is removed from the right side of (5.4a), then only the Newtonian field is considered such that integration has the exact form:

$$\begin{aligned} e^{-\lambda} &= 1 - \left(\frac{2a_o r_c}{c^2 R} \right) [2.5 (1 - \exp(-R))] \\ &= 1 - \left(\frac{2GM_{\max}}{c^2 r_c R} \right) [(1 - \exp(-R))] \end{aligned} \quad (5.4e)$$

We can derive some properties of this field by considering tensor component T_4^4 in equation (5.3c) expressed in terms of $e^{-\lambda}$:

$$8\pi \left(\frac{G}{c^4} \right) T_4^4 = -\frac{1}{r^2} \frac{d}{dr} \left\{ r \left(e^{-\lambda} - 1 \right) \right\}, \quad (5.5)$$

which with (5.4e) evaluates to:

$$T_4^4 = \left(\frac{M_{\max} c^2}{4\pi r_c} \right) \left(\frac{\exp(-r/r_c)}{r^2} \right). \quad (5.6)$$

This *equivalent* energy density is not proportional to the bulk density (5.1c) because the galactic matter is suspended by orbital angular momentum which has not been included. For the total field (5.4c) substituted in (5.5), we get for small r :

$$T_4^4 \approx \left(\frac{M_{\max} c^2}{4\pi r_c} \right) \left(\frac{4.5 \exp(-r/1.5r_c)}{r^2} \right). \quad (5.8)$$

This is an equivalent energy density because the real mass density is still given by (5.1c).

6. Application to gravitational lenses

Since many examples of gravitational lenses have been observed to imply the presence of dark matter, it will be assumed that the gravito-cordic field also causes light deflection analogous to normal gravity, [26]. In the simplest configuration for producing a standard Einstein ring from a distant point source the observed ring angular radius is:

$$\theta_M \approx 4 \frac{GM}{c^2 R}, \quad (6.1)$$

where M is the compact lens mass consisting of *observable* matter and R is the exterior impact parameter. If the distant source is off-axis, then two arcs or two smaller images of comparable brightness will be produced at separation around $2\theta_M$. When light from a distant source passes *through* a galaxy or cluster, calculation of its deflection is somewhat more complicated than this exterior case. Figure 2 illustrates this situation where M_R is the observable mass included within the impact parameter R . In particular, the *total* gravitational potential within a body is the sum of exterior and interior parts:

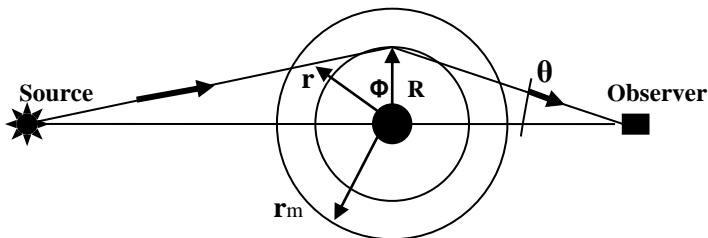


Figure 2. Schematic diagram for deflection of light from a distant source passing *through* a massive cluster.

(i) The outer edge of the body (radius r_m) is at a negative potential relative to infinity such that the potential function at the exterior surface is:

$$\left(e^{-\lambda}\right)_{\text{Ext}} \approx 1 - 2GM_m/c^2 r_m \quad . \quad (6.2)$$

(ii) Within the cluster, the interior potential is due to the field of (3.6) and is derivable from:

$$\left(\frac{c^2}{2}\right) \frac{d}{dr} \left(e^{-\lambda}\right)_{\text{Int}} \approx g_\omega = g_N + a_o \left\{ \frac{(g_N/a_o)^{1/2}}{[(g_N/a_o) + 1]} \right\} \quad . \quad (6.3)$$

Let the cluster mass be roughly proportional to radius, ($M = Qr$ where Q is a constant), then upon integration the potential function *referred to the surface* at r_m is:

$$\begin{aligned} \left(e^{-\lambda}\right)_{\text{Int}} \approx & 1 - \left[\frac{2GQ}{c^2} \ln\left(\frac{r_m}{r}\right) \right] - \\ & \left(\frac{4GQ}{c^2} \right) \left[\left(\frac{a_o r_m}{GQ} \right)^{1/2} \left(1 - \left(\frac{r}{r_m} \right)^{1/2} \right) + \tan^{-1} \left(\frac{GQ}{a_o r_m} \right)^{1/2} - \tan^{-1} \left(\frac{GQ}{a_o r} \right)^{1/2} \right] . \end{aligned} \quad (6.4)$$

Now the deflection of light may be derived from consideration of “action”. According to the geodesic equations ([25] p207), a unit of angular momentum in the local frame is equivalent to $(e^{-\lambda})$ units in the coordinate frame. However, a unit of action (say, angular momentum x angle) has to be covariant within a given body. Consequently, unit angle in the local frame is seen as increased to (e^λ) units in the coordinate frame. This slight increase represents the deflection of light phenomenon such that total deflection within a cluster is given by:

$$\theta \approx 2 \int_{r=R}^{r=r_m} (e^\lambda - 1) d\phi \quad ; \quad (6.5)$$

where R is the impact parameter, and from the geodesic equations we have:

$$d\phi \approx Rdr/r(r^2 - R^2)^{1/2} \quad . \quad (6.6)$$

Thus, for the weak field case using (6.4) we have deflection within the cluster consisting of the separate Newtonian and gravito-cordic components:

$$\theta \approx 2 \int_{r=R}^{r=r_m} \left\{ \left[\frac{2GQ}{c^2} \ln \left(\frac{r_m}{r} \right) \right] + \left[\left(\frac{4GQ}{c^2} \right) \left(\frac{a_o r_m}{GQ} \right)^{1/2} \left(1 - \left(\frac{r}{r_m} \right)^{1/2} \right) + \tan^{-1} \left(\frac{GQ}{a_o r_m} \right)^{1/2} - \tan^{-1} \left(\frac{GQ}{a_o r} \right)^{1/2} \right] \right\} d\phi . \quad (6.7)$$

Outside the cluster, the deflection calculated using (6.2) for ($r = r_m$ to ∞) is relatively negligible compared with using (6.4). However, Figure 3 illustrates the significant interior deflection calculated from (6.7), for a particular Q value of 100 galaxies ($10^{13} M_\odot$) within radius 1Mpc. Light passing through this size of cluster is therefore deflected mainly by the gravito-cordic field, unless there really is a proportion of dark matter not included here.

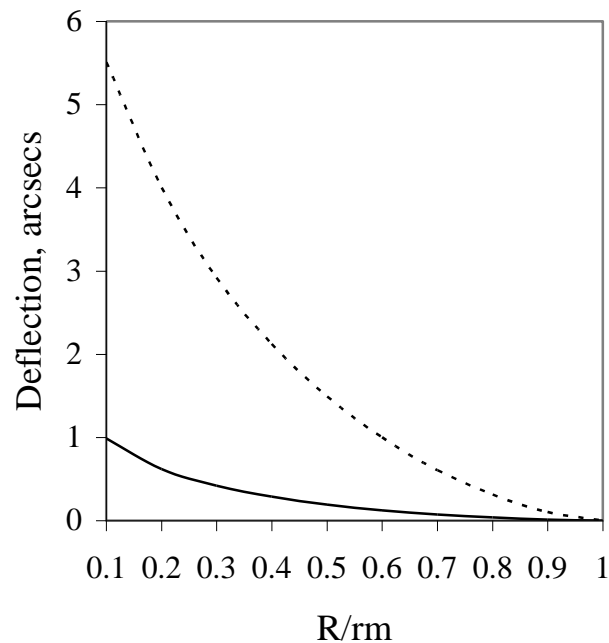


Figure 3. The calculated relativistic deflection of light travelling through a galactic cluster due to the Newtonian component (—), and the gravito-cordic component (- - -). Cluster size has been fixed at a typical value, $r_m = 1\text{Mpc}$, and $Q = M/r = 10^{13}M_\odot / \text{Mpc}$.

If the deflection of light were calculated in the normal way using the geodesic equations, absolute potential would be employed through the cluster. Thus, from (6.2) and (6.4), the potential function is:

$$\left(e^{-\lambda} \right)_{\text{abs}} \approx [1 - 2GQ/c^2] + \left[\left(e^{-\lambda} \right)_{\text{int}} - 1 \right] , \quad (r < r_m) . \quad (6.8)$$

And from the geodesic equations, the photon trajectory is given by:

$$\frac{d^2u}{d\phi^2} + u(e^{-\lambda})_{\text{abs}} + \frac{1}{2}u^2 \frac{d}{du}(e^{-\lambda})_{\text{abs}} = 0 \quad , \quad (6.9)$$

where $u = 1/r$. Numerical integration produces the same total deflection as already given.

One important point to be emphasised is that the gravito-cordic field does not exist outside a galaxy or cluster where there is no orbiting material, so no concomitant deflection of light can occur there. This contrasts with Milgrom's, Bekenstein's and Moffat's theories which modify normal gravity out to infinite radius.

7. Quantisation effects

7.1 Resonance in galactic orbits

It is thought that the gravito-cordic field induces resonance in disc galaxy orbits, resulting in flat rotation curves, disc stability, and bar or spiral structures. Hydrogen atoms will be proposed as the main source of the gravito-cordic field because their corresponding *gravitational de Broglie wavelength* shows a special fit to galactic dimensions, as follows. Given that the normal electromagnetic de Broglie wavelength for electrons of velocity v is defined as

$$\lambda = h / mv \quad , \quad (7.1)$$

we shall propose that hydrogen atoms in galaxies emit a gravito-cordic field with a *gravitational de Broglie wavelength*:

$$\lambda_{\text{GH}} = \left(\frac{h}{mV} \right) \times 137 \times \left(\frac{e^2}{Gm^2} \right)^{1/2} \quad . \quad (7.2)$$

This is to be the *quantisation wavelength* of the gravito-cordic field which organises galactic hydrogen into discrete orbits, nodes and clumps. Factor 137 is the inverse atomic fine structure constant, (e^2/Gm^2) is the ratio of electric to gravitational force, h is Planck's constant, m the hydrogen-electron mass and V is the local galactic rotation velocity.

For a particular galactic mass ($M_G = 1.09 \times 10^{11} M_\odot$), and average rotation velocity ($V \approx 201 \text{ kms}^{-1}$) for Sa,b,c galaxies, we find a remarkable theoretical coincidence given earlier in (2.2):

$$2\pi \left(GM_G / c^2 \right) \approx \lambda_{\text{GH}201} \quad . \quad (7.3)$$

Let mass M_G reside within radius R_G , and put $n_G = c / V_{201}$ in order to get an expression for the number of quantisation wavelengths around this circular orbit:

$$\frac{2\pi R_G}{\lambda_{GH201}} = n_G^2, \quad (7.4)$$

which is around 2.2 million. The particular galactic velocity [$V = 201 \text{ km s}^{-1} = (4\pi / 137^2)c$] will be investigated in detail elsewhere because it has a special electromagnetic relationship with the hydrogen 1st Bohr orbit velocity ($v_1 = c/137$).

Now, given this relationship between quantisation wavelength and orbit circumference, we can propose a mechanism which produces *constant* orbital velocity over a wide range of galactic radii. Consider Figure 4 which illustrates three adjacent orbits, each satisfying the *general de Broglie* conditions (7.2):

$$2\pi r = N\lambda_{GH}, \quad (7.5)$$

such that $N_B = N_A + 1 = N_C - 1$. Let material at B emit a gravito-cordic field counter-clockwise azimuthally in the direction B1 so as to satisfy quantisation condition (7.5), but let the field also spread to affect orbits A and C to some extent. Then for $N \gg 1$, and the given orbit radial separation ($\lambda_{GH}/2\pi$), the length of the path taken by the field from B around to C is:

$$L_{BC} \approx N_B \lambda_{GH} + \lambda_{GH} / 2. \quad (7.6)$$

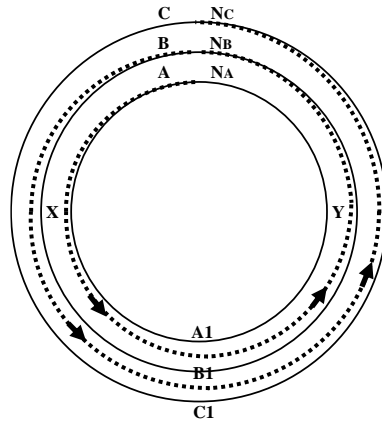


Figure 4. Three adjacent orbits A, B, C, in a disc galaxy, each satisfying the de Broglie condition ($2\pi r = N\lambda_{GH}$). Due to coherence, a two-armed structure is produced through C,B,A - A1,B1,C1.

Similarly, the spiral orbit for a field travelling from B around to A is approximately of length:

$$L_{BA} \approx N_B \lambda_{GH} - \lambda_{GH} / 2 \quad . \quad (7.7)$$

That is, if A, B and C just happen to be in phase, then the field from B will assist the native field in orbits A and C, given that there are two stable node positions per λ_{GH} (at phase zero and π for an *intensity* field). The field from B will be in *anti-phase* to that in orbits A or C at positions X and Y; however, over much of the orbit the fields are partially in phase. Now coherence represents the overall lowest energy state so there will be a tendency for adjacent orbits to resonate at the same quantisation frequency (c / λ_{GH}), as the field coerces material towards a single orbital velocity V. Original node alignment could be established by random clumping of matter at A say, which then encourages matter at B and C to shift into phase by the above process. For each complete wavelength there are two stable intensity nodes, so there will be a stable potential valley at A1, B1, C1, etc. Consequently, a *two armed material structure* is eventually produced which, if uninfluenced by differential rotation, would extend straight to the edges of the galaxy as a bar. Alternatively, shearing viscosity forces produce a two-armed spiral. In conclusion, there are quantisation forces inherent to the gravito-cordic field trying to usher matter into a diametrical structure, leaving regions of least coherence at X and Y relatively deficient in matter. Density-wave theory [31-33] will probably apply at the same time in harmony with the actual material distribution.

It is understood that the spiral pattern in galaxies rotates rigidly while disc stars pass through the spiral. Furthermore, the spiral matter is usually less than 10% of the disc mass and comprises gas and dust swept from the disc, plus an enhanced density of disc stars. The effect is that of a gravitational potential valley due to enhanced mass density, which is self-perpetuating by self-gravity to some extent. Measurements of spirals reveal that some matter flows *along* the arms because the arms tend to disturb the through-flowing matter from the circular velocity needed to support it centrifugally against the gravity of the inner disc stars. But the majority of the spiral matter must have the normal disc velocity in circular orbits, with the spiral pattern merely delineating a region of enhanced mass density rather than a separate structure rotating through the disc material.

The observed branching and segmentation of grand spirals is found to be consistent with this model of circumferential quantisation nodes, as follows. Matter will accumulate in other energy node-lines as well as the grand spiral, thereby producing inter-arm branches or short inclined parallel segments within the grand spiral. [The clumping of material at nodes in an electromagnetic standing wave field has been very well demonstrated, [34]]. Figure 5 part (a) illustrates M51 with one such branch marked for analysis. The arm/branch intersection region is magnified in part (b) to reveal the proposed myriad of quantisation nodes at a particular instant. Line APB represents the *circular* orbit through P with the nodes spaced at $\lambda/2$ intervals, (typically a few million per orbit according to (7.4)). Adjacent circular quantised orbits, wx, yz for example, are $(\lambda/2\pi)$ apart and their nodes are displaced laterally along the spiral arm from those in APB due to the shearing forces. Thus, the main spiral arm at P lies at 23deg from circular

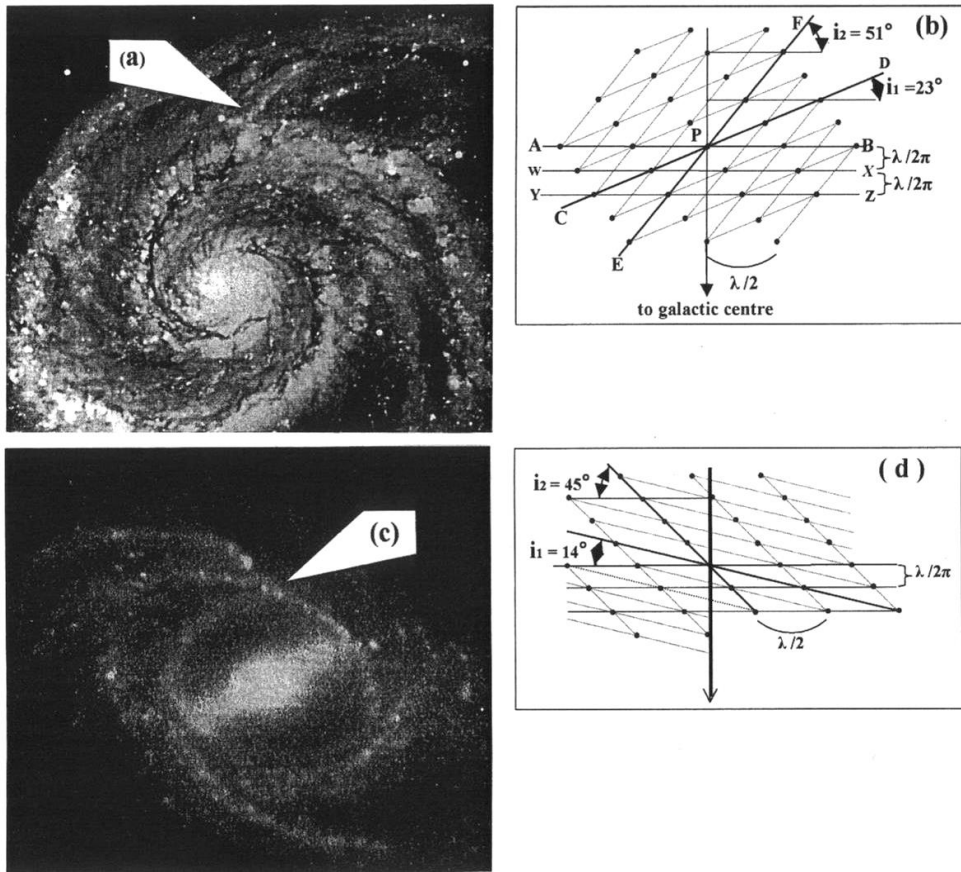


Figure 5. The proposed quantisation node pattern for two galactic spiral arm/branch intersection regions, marked in the photographs. The galactic material in both the main spiral and branch is seen to be aligned along the node lines. Parts a, b, M51; parts c, d, NGC2523.

and has tangent CPD which joins nodes of the same phase. At the same time, the branch tangent EPF lies at 51deg from circular and also joins nodes of similar phase. The figure shows the essential angles and distances involved drawn to scale such that angles i_2 and i_1 are simply connected by:

$$\cot(i_2) = \cot(i_1) - \pi/2 \quad . \quad (7.8a)$$

The barred galaxy NGC2523 has an inner ring and a strongly bifurcated spiral arm, see Figure 5 part (c). After correction for inclination of the galaxy, part (d) shows the proposed nodal pattern at the fork where the spiral arm lies at 14deg from circular and the branch lies at 45deg, so that these angles are related by:

$$\cot(i_2) = \cot(i_1) - \pi \quad . \quad (7.8b)$$

In these galaxies, quantisation theory is strongly supported by the fact that the material clearly prefers the lines of nodes rather than smeared multiple intermediate angles.

7.2 Galactic rings

Galactic rings have been analysed in terms of resonances but some problems of origin remain [35]. In particular, their *absolute* sizes still require explanation and can now be covered by gravito-cordic theory as follows. Equation (7.4) with the help of (7.2) may be generalised for any velocity V and radius r to:

$$2\pi r = N_R \lambda_{GH} (n_G^2) \quad , \quad (7.9a)$$

which also means:

$$mVr = N_R (mV_{201}R_G) \quad , \quad (7.9b)$$

where N_R is a multiple of (1/2), because there are 2 stable nodes per wavelength. Visible *outer-rings* have been observed in several galaxies: e.g. Hubble Atlas NGC2217, 2859, 3081, 3504, 4274, and 4612, [43]. The rings are sometimes broken and superimposed by spiral arm segments, and are not entirely separated from the galactic disc or lens structure. Nevertheless, a gap of reduced brightness inside the ring implies that the ring material is in a preferred orbit compared with the gap material. It is clear from the photographs that N_R is very low because the ring is often diffuse and solitary. Kormendy [36] has remarked that outer rings are unusually rich in HI so λ_{GH} is most appropriate here. All these rings are real and not related to the phantom dark matter rings described by Milgrom and Sanders [72].

Table 1 lists some outer-ring galaxies for which good rotation data are available. Galactic type and radius are mainly from de Vaucouleurs and Buta [37]. Quantum number values N_R are our main concern, and they are seen to lie preferentially around unity. Galaxies NGC1068, 1291, 1326, 2859, 4736 and 5701 are similar in that their outer-ring structure appears joined to the central lens/bar by two wide spiral arms, and the type of central region is apparently unimportant. NGC4394 has an outer-ring which is more clearly a part of the outer disc. Similarly, the outermost arms of NGC1300 bend purposefully to form an outer-ring rather than a logarithmic spiral pattern. Galaxy NGC 7217 has a strong ring structure and the spiral arms are segmented but traceable across the low surface brightness ring; so the process of segmentation continues at the same time as the ring processes.

Table 1. Quantum numbers N_R for some galaxies with outer-rings.

Galaxy	Type	Distance D. Mpc	Inclin. i. deg	Radius arcmin,kpc	$v \sin i$ kms ⁻¹	v kms ⁻¹	N_R	Ref
N1068	RSA(rs)b	22.0	40	2.5, 16.0		200	1.36	[50]
N1291	RSB(s)o	13.8	6	4.1, 16.5	20	190	1.34	[44]
N1326	RLB(r)	24.5	40	1.4, 10.0	130	202	0.86	[44]
N2859	RLB(r)	31.0	27	1.7, 15.3	85	187	1.22	[45]
N3419	RLAB(r)	58.0	31	0.55, 9.3	120	233	0.92	[45]
N3626	RLA(rs)	29.5	45	0.70, 6.0	173	245	0.63	[46]
N4321	SAB(s)bc	20.0	35	2.5, 14.6		204	1.27	[47]
N4394	RSB(r)b	18.9	22	1.4, 7.7	84	224	0.73	[48]
N4736	RSA(r)ab	6.1	32	5.6, 9.9	106	200	0.84	[48]
N5633	RSA(rs)b	46.6	58	0.95, 12.9	167	197	1.08	[48]
N5701	RSB(rs)o	30.2	21	1.8, 15.8	65	181	1.22	[48]
N1300	SB(rs)bc	30.9	40	2.7, 24		160	1.64	[49]
N2217	RLB(rs)	32.4	32	1.6, 15.1	135	225	1.45	[48]
N4274	RSB(r)ab	18.6	72	2.9, 15.7	226	238	1.59	[46]
				1.32, 7.2	226	238	0.73	[46]
N5101	RSB(rs)o	33.7	27	2.5, 24.5	95	209	2.18	[70]
				0.85, 8.3	95	209	0.74	[71]
N7217	RSA(r)ab	24.5	33	1.25, 8.9	155	285	1.08	[51]
				0.55, 3.9	159	292	0.49	[51]

In general, the observed diffuse nature of outer-rings is a measure of the weakness of the quantisation field relative to turbulence forces. It is an intensity field, so there are no forbidden zones. When a spiral is superimposed on a ring, both ring and spiral-forming mechanisms must operate simultaneously. Furthermore, it does not seem to matter whether there is a bar or just a lens at the centre of these galaxies.

Table 2. Quantum numbers N_H for galaxies with rings of HI.

Galaxy	Distance	Inclin. i. deg	Radius	Velocity	N_H	Ref
	D. Mpc		r_1, r_2, r_3 kpc	v_1, v_2, v_3 kms ⁻¹		
N224	0.69	78	6.0, 11.0, 17.0	200, 260, 240	0.51, 1.2, 1.7	[52]
N224	0.69	78	6.0, 10.5, 17.0	250, 245, 225	0.6, 1.1, 1.6	[53]
IC342	4.50	25	5.0, 9.0, 15.0	155, 190, 200	0.33, 0.7, 1.3	[54]
IC342	4.50	25	5.0, 14.0, 25.0	160, 190, 190	0.34, 1.1, 2.0	[55]
N628	15.0	6	4.4, 15.0, 22.0	200, 230, 250	0.37, 1.5, 2.3	[56]
N891	14.0	90	2.8, 9.4, 16.3	160, 225, 225	0.2, 0.9, 1.6	[57]
N2841	13.5	60	5.0, 12.0, 30.0	270, 290, 265	0.58, 1.5, 3.4	[58]
N3031	3.30	59	3.5, 7.5, 11.0	210, 235, 205	0.31, 0.8, 1.0	[59]
N3938	16.0	9.5	2.3, 7.0, 10.3	150, 230, 230	0.15, 0.7, 1.0	[60]
N4203	21.6	35	22.1	210	2.0	[61]
N4258	6.60	72	10.0, 17.0, 24.0	200, 200, 200	0.85, 1.4, 2.0	[62]
N4278	16.4	45	4.0, 12.0	212, 254	0.36, 1.3	[63]
N5236	8.90	18	3.6, 6.7, 9.1	180, 230, 240	0.28, 0.7, 0.9	[64]
N5457	7.20	18	4.0, 10.0, 16.0	190, 220, 200	0.32, 0.9, 1.4	[65]
N5457	6.90	22	5.0, 10.0, 16.0	130, 185, 200	0.28, 0.8, 1.4	[54]
N5905	71.0	40	20, 31.0, 45.0	220, 230, 240	1.9, 3.0, 4.6	[66]
N6946	10.1	30	4.0, 7.5, 11.0	130, 180, 205	0.22, 0.6, 1.0	[54]
N7013	23.0	72	11.5	158	0.77	[67]
N7331	22.0	75	8.0, 13.0, 18.0	230, 225, 225	0.78, 1.2, 1.7	[68]
Galaxy			4.0, 9.0, 14.0	215, 253, 250	0.37, 1.0, 1.5	[69]

Many galaxies have no visible rings but contain broad rings of neutral hydrogen extending over a range of quantum numbers; thereby indicating that *self-gravity* of the neutral hydrogen has caused the less-preferred zones to fill-up. Table 2 lists several galaxies with broad HI rings. Characteristic radii are given on either side of the peak density in order to derive the corresponding range of quantum numbers N_H , which are seen to be around 1 or 2.

Far-infrared observations of cold dust in M31 [38] have revealed two striking rings which fit quantum numbers $N_H \approx 1.0$ and 1.5. Evidently, the dust appears to be associated with hydrogen which is governing the ring parameters.

7.3 Systems obeying the J proportional to M^2 law

The J proportional to M^2 law originally reported by Brosche [39] has been proposed by Wesson [40,41] as evidence of self-similarity between the various groups of bodies. According to gravito-cordic quantisation theory herein, an explanation for this observed law proceeds from the early Universe in which vast clouds of turbulent gas constituted the expanding material at that time.

As mentioned in Section 7.1, there is theoretically an optimum material velocity for implementing the gravito-cordic quantisation phenomenon in hydrogen, namely:

$$v_z = (4\pi/137^2)c \approx 201 \text{ kms}^{-1}. \quad (7.10)$$

It is possible then that turbulent material volumes of galactic proportions may have separated-out within the general expansion when they had this preferred rotation velocity, and were self-supporting so that:

$$GM \approx v_z^2 r_z . \quad (7.11)$$

Thus, at the point of separation we can write for each spherical element,

$$v_z \approx [G\rho(4/3)\pi]^{1/2} r_z , \quad (7.12)$$

where ρ is the average gas density in the element, and $M = (4/3)\pi\rho r_z^3$. Variation in ρ allowed a wide range of galactic masses to be produced. If the total universal material of mass 10^{52} kg only consisted of such adjacent elements, then the separation occurred at around 10^8 years from the beginning.

Given that velocity v_z is preferred, then after separation the total angular momentum of a randomly rotating spherical element is

$$J \approx (3/5)M v_z r_z , \text{ or } J \approx p M^2 . \quad (7.13)$$

Here p is a constant equal to $(3/5)(G/v_z)$ which has the value drawn on Figure 6, namely:

$$p_{201} = 2.00 \times 10^{-15} \text{ g}^{-1} \text{ cm}^2 \text{ s}^{-1} , (2.00 \times 10^{-16} \text{ kg}^{-1} \text{ m}^2 \text{ s}^{-1}) . \quad (7.14)$$

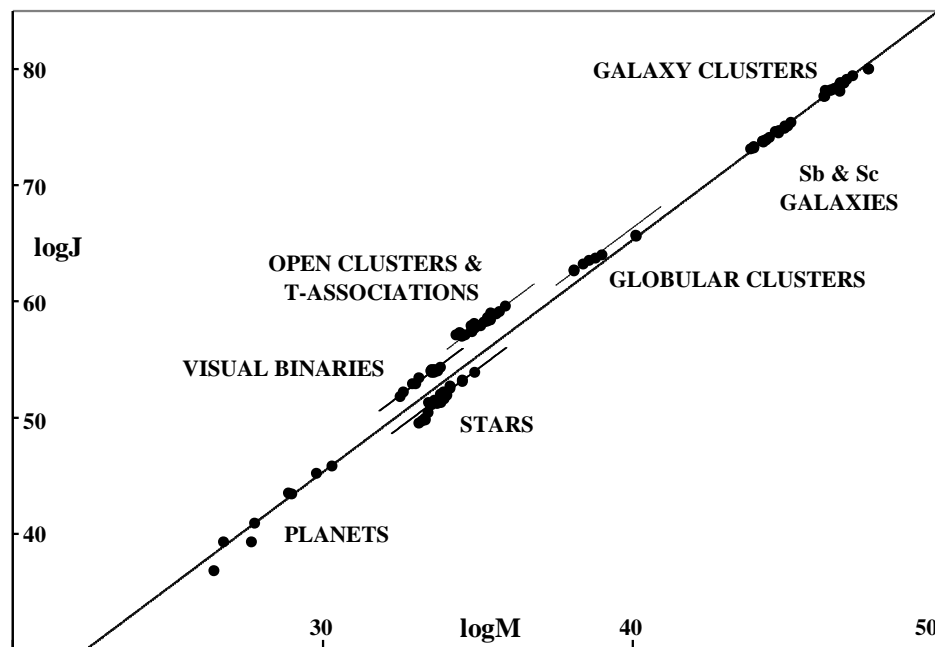


Figure 6. The angular momentum versus mass relationship for various astronomical bodies, showing a theoretical straight line for $J = 2.00 \times 10^{-15} M^2$ over 40 decades.

Although some *galaxies* may have formed like this from the early denser gas content, the more massive *cluster* formation would have commenced later (when ρ was lower) if (7.11) and (7.12) were again involved. For example, v_z could represent the circular component of the dispersion velocity in turbulent material, then adjacent clusters of mass $10^{13} M_\odot$ would have separated at 2.5×10^9 yr. The total expanding field then consisted of numerous separate cluster-volumes, each of which obeyed (7.13) approximately. There could have been a difference in the type of galaxy which formed before or after the *cluster* separation. For example, the early denser material was probably more turbulent, leading to more rapid star formation and evolution in elliptical galaxies: in contrast to spiral galaxy production by agglomeration of matter within calmer clusters.

Table 3. Proportionality constant $p = J / M^2$, for astronomical bodies.

<u>Planets</u>	<u>p</u>	<u>Visual Binaries</u>	<u>p</u>	<u>Sc Galaxies</u>	<u>p</u>
Mercury	6.00×10^{-17}	η Cas	14.4×10^{-14}	I467	2.71×10^{-15}
Earth	1.98×10^{-15}	O ² Eri BC	14.0 "	N1087	2.94 "
Mars	5.02×10^{-15}	ξ Boo	10.1 "	N1421	1.98 "
Jupiter	1.90×10^{-15}	70 Oph	8.39 "	U2885	1.46 "
Saturn	4.37×10^{-15}	α Cen AB	7.63 "	N2998	1.97 "
Uranus	4.22×10^{-15}	Sirius	4.69 "	U3691	3.08 "
Neptune	2.22×10^{-15}	Kru 60	9.89 "	N4321	1.96 "
Pluto	8.54×10^{-17}	Procyon	4.53 "	N7664	2.25 "
		ζ Her	5.80 "		
		85 Peg	5.65 "		
		Ross 614AB	8.69 "		
		Fu 46	6.37 "		
<u>Stars</u>				<u>Sb Galaxies</u>	
dO5	1.19×10^{-16}			N1085	1.33×10^{-15}
dB0	1.25 "			N1417	1.44 "
dB5	1.65 "	<u>Open clusters</u>		N1515	2.65 "
dA0	1.97 "			N2815	1.52 "
dA5	1.82 "			N3200	1.46 "
dF0	1.00 "	M103	9.35×10^{-13}	N7083	1.85 "
dF5	0.30 "	XPer	5.53 "	N7537	2.23 "
dG0	0.16 "	Stock 2	4.69 "	U12810	1.73 "
dG5	0.17 "	M34	5.91 "		
dK0	0.17 "	Pleiades	4.18 "		
dK5	0.18 "	Hyades	5.13 "		
gB0	1.23 "	M36	7.91 "	<u>Galaxy clusters</u>	
gB5	2.37 "	M37	4.58 "	Virgo	0.66×10^{-15}
gA0	3.49 "	τ CMa	7.25 "	PegI	1.78 "
gF5	2.37 "	N3532	5.31 "	Pisces	5.75 "
gG0	0.70 "	M21	7.24 "	Cancer	2.75 "
gG5	0.53 "	M11	6.24 "	Perseus	1.95 "
gK0	0.67 "	M39	7.20 "	Coma	1.70 "
gK5	0.84 "			UMaIII	2.19 "
		<u>T-associations</u>		Hercules	0.52 "
<u>Globular clusters</u>				ClusterA	1.66 "
N104	9.98×10^{-15}	Tau T1	19.8×10^{-13}	Centaurus	2.82 "
M3	18.0 "	Tau T2	28.8 "	UMaI	1.74 "
M5	32.6 "	Aur T1	28.4 "	Leo	1.74 "
M4	28.2 "	Ori T1	21.0 "	Gemini	2.09 "
M13	13.9 "	Ori T2	6.26 "	Cor.Bor.	1.48 "
M92	19.4 "	Mon T1	12.5 "	ClusterB	1.78 "
M22	2.60 "	Ori T3	12.8 "	Bootes	2.51 "
M15	3.11 "	Sco T1	24.3 "	UMaII	1.82 "
		Per T2	9.87 "		

The data plotted in Figure 6 and listed in Table 3 have representative dimensions from Allen [42]. For *clusters of galaxies* the data give a mean value of $p = 1.95 \times 10^{-16} \text{ kg}^{-1}\text{m}^2\text{s}^{-1}$ corresponding to a dispersion velocity circular component of 206 km s^{-1} . Likewise, the data for *Sb and Sc disc galaxies* correspond to an average peripheral velocity of 202 km s^{-1} in good agreement with quantisation theory. The five other systems show angular momentum proportional to mass-squared and their different constants of proportionality will be found (in a later paper) to correspond to *preferred* quantisation wavelengths fitting the particular dimensions of those systems. This establishes some control in the creation of astronomical bodies as a whole. Definite gaps exist between the classes because suitable quantisation rules cannot be established there. No classical explanation exists for these gaps, nor for the specific sizes of existing bodies.

8. Conclusion

An auxiliary gravitational field has been proposed in order to account for the empirical success of Milgrom's MOND theory without actually modifying normal gravity. This azimuthal gravito-cordic field energy belongs to the orbiting material and is induced into existence by the normal radial gravitational field from included matter. Interaction between these fields constitutes the additional gravitational force necessary to support the extraordinary velocities seen in apparently mass-deficient galaxies. The gravito-cordic field is a little stronger than the MOND field and can reduce the mass-to-light ratio by 15% further. In addition, the field has a standing-wave nature which induces resonance in disc galaxies resulting in flat rotation curves plus bar or spiral structures, segmentation of material, and galactic rings. Preference for an optimum velocity (201kms^{-1}) during galaxy creation in the early universe has also made their angular momentum proportional to mass-squared on average.

Acknowledgements

I would like to thank Imperial College Library Staff, R. Glovnea for computing assistance and R. Simpson for typing.

References

1. Milgrom M: *Astrophys J* 1983, **270**:365.
2. Milgrom M: *Astrophys J* 1983, **270**:371.
3. Milgrom M: *Astrophys J* 2002, **577**:L75.
4. Milgrom M: *New Astron Rev* 2002, **46**:741
5. Sanders RH: *Mon. Not. R. Astr Soc* 1986, **223**:539.
6. Sanders RH: *Astrophys J* 1996, **473**:117.
7. Sanders RH: *Astrophys J* 1999, **512**:L23.
8. Begeman KG, Broeils AH, Sanders RH: *Mon Not R Astr Soc* 1991, **249**:523.
9. McGaugh SS, de Blok WJG: *Astrophys J* 1998, **499**:66.
10. de Blok WJG, McGaugh SS: *Astrophys J* 1998, **508**:132.
11. Sanders RH, Verheijen MAW: *Astrophys J* 1998, **503**:97.
12. Sanders RH, McGaugh SS: *Ann Rev Astron Astrophys* 2002, **40**:263.
13. Sanders, RH: *arXiv:astro-ph/0601431v2*
14. Milgrom M, Sanders RH: *Astrophys J* 2007, **658**:L17.
15. Fisher JR, Tully RB: *Astrophys J Suppl Ser* 1981, **47**:139.
16. Bekenstein JD: *Phys Rev D* 2004, **70** 083509.
17. Moffat, JW: *arXiv:astro-ph/0608675*.
18. Moffat, JW: *arXiv:gr-qc/0506021*.
19. Sanders RH: *Mon Not R Astr Soc* 2006, **370**:1519.
20. Terman FE: *Electronic & Radio Engineering*, 4th Ed, McGraw-Hill 1955, p67.
21. Kent SM: *Astron J* 1986, **91**:1301.
22. Kent SM: *Astron J* 1987, **93**:816.
23. Kent SM: *Astron J* 1988, **96**:514.
24. Brownstein JR, Moffat JW: *Mon Not R. Astr Soc* 2006, **367**:527.
25. Tolman RC: *Relativity Thermodynamics and Cosmology*, Clarendon Press 1934.
26. Mortlock DJ, Turner EL: *Mon Not R Astr Soc* 2001, **327**:557.
27. Inada N, *Nature* 2003, **426**:810.
28. Maoz D: *Astrophys J* 1997, **486**:75.
29. Takahashi R, Chiba T: *Astrophys J* 2001, **563**:489.
30. Wambsgans J, Renyue C, Ostriker J P, Turner EL: *Science* 1995, **268**:274.
31. Lin CC, Shu FH: *Proc Nat Acad Sci* 1966, 55:229.

32. Lin CC: in *The spiral structure of our Galaxy*, ed. Becker W, Contopoulos G: Dordrecht: Reidel; 1970:373.
33. Shu FH, Stachnik RV, Yost JC: *Astrophys J* 1971, **166**:465.
34. Zemanek P, Jona A, Sramek L, Liska M: *Optics Comm* 1998, **151**:273.
35. Buta R, Combes F: *Fundamentals of cosmic physics* 1996, **17**:95.
36. Kormendy J: *Astrophys J* 1979, **227**:714.
37. de Vaucouleurs G, Buta R: *Astron J* 1980, **85**:637.
38. Haas M, et al: *Astron Astrophys* 1998, **338**:L33.
39. Brosche P: *Astrophys Space Science* 1978, **57**:463.
40. Wesson PS: *Astron Astrophys* 1979, **80**:296.
41. Wesson PS: *Phys Rev D* 1981, **23**:1730.
42. Allen CW: *Astrophysical Quantities, 3rd edition*, London: Athlone Press; 1973.
43. Sandage A: *The Hubble atlas of galaxies* Washington, D.C.:Carnegie Inst; 1961.
44. Mebold U, et al: *Astron Astrophys* 1979, **74**:100.
45. Biegging JH, Biermann P: *Astron Astrophys* 1977, **60**:361.
46. Krumm N, Salpeter EE: *Astrophys J* 1979, **228**:64.
47. Rubin VC, Thonnard N, Ford WK: *Astrophys J* 1980, **238**:471.
48. Bottinelli L, Gouguenheim L, Paturel G: *Astron Astrophys Sup Ser* 1982, **47**:171.
49. Peterson CJ, Huntley JM: *Astrophys J* 1980, **242**:913.
50. Scoville NZ, Young JS, Lucy LB: *Astrophys J* 1983, **270**:443.
51. Peterson CJ, et al: *Astrophys J* 1978, **219**:31.
52. Gottesman ST, Davies RD: *Mon Not R Astr Soc* 1970, **149**:263.
53. Emerson DT: *Mon Not R Astr Soc* 1976, **176**:321.
54. Rogstad DH, Shostak GS: *Astrophys J* 1972, **176**:315.
55. Newton K: *Mon Not R Astr Soc* 1980, **191**:169.
56. Shostak GS, van der Kruit PC: *Astron Astrophys* 1984, **132**:20.
57. Sancisi R, Allen RJ: *Astron Astrophys* 1979, **74**:73.
58. Bosma A: *Astron J* 1981, **86**:1791.
59. Rots AH, Shane WW: *Astron Astrophys* 1975, **45**:25.
60. van der Kruit PC, Shostak GS: *Astron Astrophys* 1982, **105**:351.
61. Burstein D, Krumm N: *Astrophys J* 1981, **250**:517.
62. van Albada GD: *Astron Astrophys* 1980, **90**:123.
63. Raimond E, Faber SM, Gallagher JS, Knapp GR: *Astrophys J* 1981, **246**:708.
64. Combes F, et al: *Astron Astrophys* 1978, **67**:L13.

65. Bosma A, Goss WM, Allen R: *Astron Astrophys* 1981, **93**:106.
66. van Moorsel GA: *Astron Astrophys* 1982, **107**:66.
67. Knapp GR, van Driel W, et al: *Astron Astrophys* 1984, **133**:127.
68. Young JS, Scoville N: *Astrophys J* 1982, **260**:L41.
69. Burton WB: *Ann Rev Astron Astrophys* 1976, **14**:275.
70. Reif K, Mebold U, et al: *Astron Astrophys Suppl Ser* 1982, **50**:451.
71. Balkowski C, Chamaraux P: *Astron Astrophys Suppl Ser* 1983, **51**:331.
72. Milgrom M, Sanders RH: *Astrophys J* 2008, **678**:131.